# Memory Subspaces for Temporal Locations Across Timescales in the Monkey Precuneus

Anonymous Author(s)


## Abstract

Understanding how the brain organizes the temporal structure of experience across different timescales is central to episodic memory. Here, we examine neural population dynamics in primate precuneus during a temporal order judgment task spanning seconds to minutes, and cross-day retrieval of intertwined episodes. We recorded large-scale population activity (∼3,000 neurons) across 3 days and analyzed it using generalized linear models and low-dimensional manifold methods. Single neurons showed consistent positive modulation for temporal locations (TLs) across both 2-s and 1-min delay conditions during retrieval. At the population level, neural activity formed structured low-dimensional manifolds in dPCA space, showing a maintained subspace with persistent encoding of TLs of the extracted frames during the TOJ period. Behavioral errors were associated with a collapse of these memory subspaces and a loss of dynamical synchrony between trajectories, while correct trials exhibited coherent, synchronized dynamics for different TLs. During cross-day retrieval, episodic states corresponding to the TL of clips viewed across both days, rapidly separated into day-specific clusters within a shared state space, and was absent in control conditions. The chronologically recent Day-2 subspace occupied a larger representational volume, which also corresponded to higher memory performance, compared to that of Day-1 clips. These results suggest that episodic time is encoded as a dynamically maintained neural manifold supporting episodic memory decisions.


## Introduction

How the brain organizes the temporal structure of experience across different timescales remains unclear (Clayton & Dickinson, 1998). Here, we examine population dynamics in primate medial posterior parietal cortex during temporal order judgments (Zuo et al., 2026) spanning seconds to minutes and across-day episodes. We propose that temporal memory is supported by a unified low-dimensional manifold whose geometric integrity and dynamical structure enable accurate retrieval.

## Methods

Two rhesus monkeys were trained on a temporal order judgment (TOJ) task using naturalistic video episodes learned across two encoding days. During a retrieval test on a third day, images sampled from all previously learned episodes were presented in pairwise comparisons. Population spiking activity was recorded from the precuneus, yielding ∼3,000 single units, and analyzed using generalized linear model (GLM), demixed principal component analysis (dPCA, Kobak et al., 2016), and nonlinear manifold geometry methods. To verify specificity, we conducted a control experiment using the same TOJ procedure with images unrelated to those encoded video episodes, recording ∼800 single units.

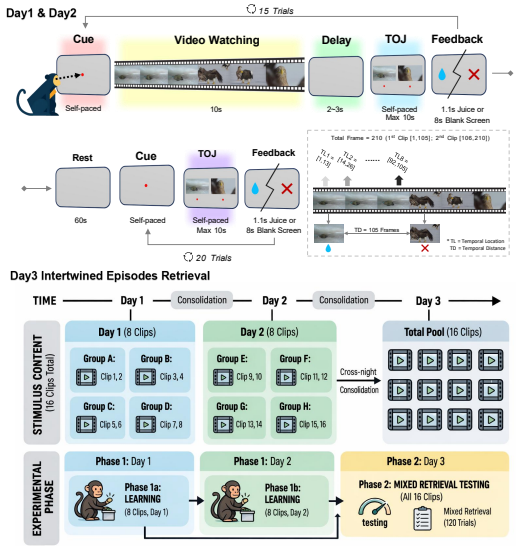


**Figure 1: TOJ memory task and three-day paradigm structure.** On *Days 1* and *2*, monkeys viewed 10-s videos (two concatenated 5-s clips). Following a 2-s delay, they performed a two-alternative forced-choice (2AFC) temporal order judgment (TOJ) on two extracted frames, identifying the earlier frame (15 trials). A 1-min retention interval preceded 20 additional TOJ trials without video play. Each day comprised four blocks with unique, unseen videos (8 clips each day). On *Day 3*, monkeys completed 120 TOJ trials integrating the full 16-clip set learned from preceding two days.

## Results

### Neural coding of temporal locations (TLs) of *frames* in memory

We ran GLMs on single neurons to examine their responses to temporal location (TL) during the TOJ phase across 2-s and 1-min delay conditions. A significant correlation was observed in a large majority of neurons in terms of Modulation weights ($\beta$) across the two delay conditions (Fig. 1A, top). This bias reflected in $\beta_{TL}$ distributions was consistently maintained across all individual

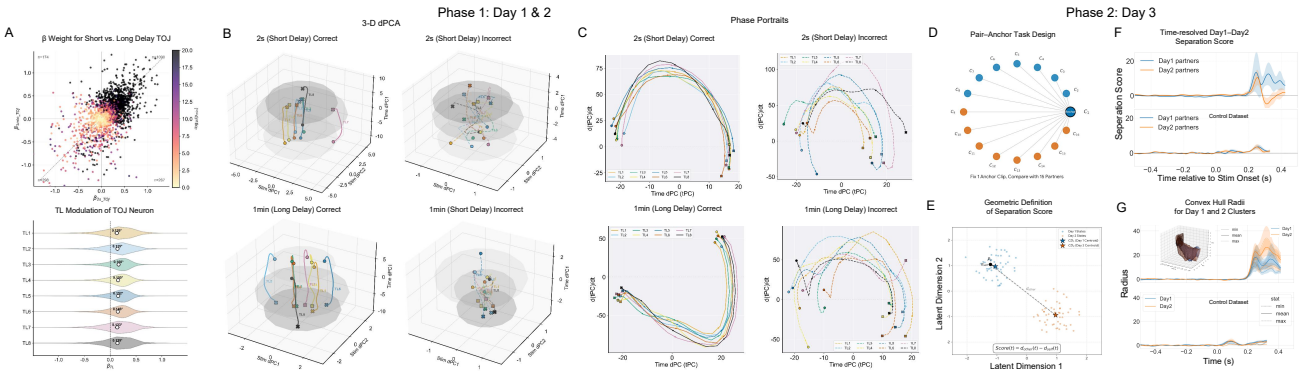


**Figure 2: Population trajectories and manifold geometry of memory subspaces encoding temporal locations of frames within days, and episodic location of clips across days. (A) Single-neuron modulation weights.** Scatterplot of GLM $\beta$ weights comparing 2-s and 1-min delay conditions. A high density of neurons in the top-right quadrant ($n$ = 1090) indicates a shared, positive-modulation encoding scheme across both temporal scales. This positive bias is consistently maintained across all individual temporal locations (TL1–TL8) encoding the location of the TOJ frame in the clip, with $\beta_{TL}$ distributions significantly shifted above zero (open circles, means; $*P < 0.05$). **(B) Low-dimensional manifold projections.** 3D dPCA-subspace trajectories for different TLs during the TOJ period, corresponding to 2-s (top) and 1-min (bottom) delays, with 2-D Stim (TL,x-y) PCs and 1 Time PC (*tPC*, z). Correct trials (left) show organized manifolds with clear TL stratification, while incorrect trials (right) show structural collapse and entanglement. The long-delay manifolds exhibited more uniform geometric motifs than short-delay ones. **(C) Phase portraits** derived from plotting the temporal derivative of the primary time-related component ($d(tPC)/dt$) against its current state (*tPC*). Correct trials (left) exhibit synchronous temporal evolution across TLs for both delay conditions. Incorrect trials (right) show desynchronized dynamics. **(D) Pair-Anchor Task Design.** Schematic of the analysis framework where neural trajectories are compared by fixing one clip as an Anchor and pairing it with 15 other Partner clips from Day 1 and Day 2. Neural population activity was organized as a neurons $\times$ conditions $\times$ time tensor and projected into a dPCA subspace fitted within a cutoff window (-0.5 s to shortest mean RT). **(E) The Definition of Separation Score.** Population activity was projected into a task-aligned dPCA subspace. For each point in each day-specific cluster, we compared their distance to the centroid of the other cluster ($d_{other}$) vs. to its own cluster ($d_{own}$) as a function of time ($d_{other}(t) - d_{own}(t)$). **(F) Separation Score dynamics.** A separation between the day clusters is seen after onset of TOJ for the main experiment (Top), but not in control experiment (Bottom). **(G) Convex Hull sizes differ for day-specific clusters in the decision window.** Convex hulls enclosing day-specific clusters show that the more recent Day-2 cluster shows a clearly larger emergent radius, which corresponds to a higher representation volume of its hull (Inset) compared to Day-1, but only for the main dataset (Top), while such robust separation dynamics are not seen in the control dataset (Bottom). Hull radius was defined as the centroid-to-boundary distance.

temporal locations (TL1–TL8) (Fig. 1A, bottom).

We projected neural activity into a dPCA subspace to examine the relationship between population-level representations and behavioral outcomes. In correct trials, population trajectories for different TLs organized into smooth, hierarchically stratified manifolds for both delay conditions, whereas in incorrect trials the manifolds collapsed, and trajectories became entangled, failing to maintain the hierarchical separation of TLs (Fig. 1B). Moreover, across both timescales, all TLs for correct trials but not incorrect trials were characterized by highly synchronous trajectories as indexed by phase portraits (Fig. 1C). This synchronized evolution reflects a stable and coherent representation of the temporal sequence, suggesting a conserved dynamical scheme to bridge temporal gaps ranging from seconds to minutes.

## Representations of cross-day TLs of *clips*

We asked whether mPPC population activity distinguishes day-context during the cross-day retrieval task. We implemented a Pair-Anchor framework in which one clip was fixed as the Anchor and paired with 15 Partner clips from Day 1 and Day 2 (Fig. 2D), and a control experiment where the TOJ frames are novel and are not sourced from the viewed clips.

We created a Separation Score between Day 1 and Day 2 clusters (Fig. 2E). Across all the points in each cluster, and averaged across anchors, the variability reveals a robust positive separation in the main experiment but not in the control dataset (Fig. 2F). There is also an asymmetry in the separation score dynamics for the two clusters, which sharply diverge after the initial peak, which led us to examine the time-varying areal occupation of each subspace (Fig. 2G, top, inset).

There is a marked difference in hull radii for the day-specific subspaces. The trajectories showed a divergence in convex-hull radius dynamics, indicating that the two conditions differed not only in centroid position but also in manifold extent and boundary expansion (while those in the control dataset do not) (Fig. 2G). This representational volume differences corresponded to differential memory performance for Day 2 vs. Day 1 clips (70.9% vs. 59.1%, $p$ = 0.001).

# Discussion

The macaque precuneal neurons represent temporal locations through a unified computational framework. The shared modulation across scales suggests a stable neuronal axis for temporal indexing (Sarkar et al., 2026). The "manifold collapse" in error trials reveals the geometric basis of behavioral failure. The combination of centroid-based separation and convex-hull radius dynamics suggests that day-dependent retrieval context shapes episodic representations at multiple geometric levels. Day 1 and Day 2 states differ not only in where their trajectories are centered, but also in how their manifolds expand over time. The null effects in the control dataset suggest that these geometric differences reflect meaningful episodic organization.

# References


Clayton, N. S., & Dickinson, A. (1998). Episodic-like memory during cache recovery by scrub jays. *Nature*, *395*, 272–4.

Kobak, D., Brendel, W., Constantinidis, C., Feierstein, C. E., Kepecs, A., Mainen, Z. F., Qi, X.-L., Romo, R., Uchida, N., & Machens, C. K. (2016). Demixed principal component analysis of neural population data (M. C. van Rossum, Ed.). *eLife*, *5*, e10989. https://doi.org/10.7554/eLife.10989.

Sarkar, A., Zuo, S., Wang, C., & Howard, M. W. (2026). "what" × "when" working memory representations using laplace neural manifolds. https://doi.org/10.7554/elife.108804.1.

Zuo, S., Wang, C., Wang, L., Jin, Z., Zhou, X., Su, N., Liu, J., McHugh, T. J., Kusunoki, M., & Kwok, S. C. (2026). Neural population dynamics and temporal context cells in macaque medial parietal cortex support temporal order memory. *PLOS Biology, in press*.